

Video Article

Revealing Dynamic Processes of Materials in Liquids Using Liquid Cell Transmission Electron Microscopy

Kai-Yang Niu, Hong-Gang Liao, Haimei Zheng

Materials Sciences Division, Lawrence Berkeley National Laboratory

Correspondence to: Haimei Zheng at hmzheng@lbl.govURL: <http://www.jove.com/video/50122>DOI: [doi:10.3791/50122](https://doi.org/10.3791/50122)

Keywords: Materials Science, Issue 70, Chemical Engineering, Chemistry, Physics, Engineering, Life sciences, Liquid cell, Transmission Electron Microscopy, TEM, In situ TEM, Single nanoparticle trajectory, dynamic imaging, nanocrystals

Date Published: 12/20/2012

Citation: Niu, K., Liao, H., Zheng, H. Revealing Dynamic Processes of Materials in Liquids Using Liquid Cell Transmission Electron Microscopy. *J. Vis. Exp.* (70), e50122, doi:10.3791/50122 (2012).

Abstract

The recent development for in situ transmission electron microscopy, which allows imaging through liquids with high spatial resolution, has attracted significant interests across the research fields of materials science, physics, chemistry and biology. The key enabling technology is a liquid cell. We fabricate liquid cells with thin viewing windows through a sequential microfabrication process, including silicon nitride membrane deposition, photolithographic patterning, wafer etching, cell bonding, etc. A liquid cell with the dimensions of a regular TEM grid can fit in any standard TEM sample holder. About 100 nanoliters reaction solution is loaded into the reservoirs and about 30 picoliters liquid is drawn into the viewing windows by capillary force. Subsequently, the cell is sealed and loaded into a microscope for in situ imaging. Inside the TEM, the electron beam goes through the thin liquid layer sandwiched between two silicon nitride membranes. Dynamic processes of nanoparticles in liquids, such as nucleation and growth of nanocrystals, diffusion and assembly of nanoparticles, etc., have been imaged in real time with sub-nanometer resolution. We have also applied this method to other research areas, e.g., imaging proteins in water. Liquid cell TEM is poised to play a major role in revealing dynamic processes of materials in their working environments. It may also bring high impact in the study of biological processes in their native environment.

Video Link

The video component of this article can be found at <http://www.jove.com/video/50122/>

Introduction

The study of chemical reactions in liquids in real time and imaging biological materials in their native environment have been of significant interests across the research fields¹⁻⁵. Due to the high spatial resolution of transmission electron microscopy (TEM), imaging through liquids using TEM has attracted a lot of attention^{4,5}. However, it has been a great challenge to image liquid samples using TEM, since the conventional microscope is operated in a high vacuum environment. In addition, liquid samples have to be thin enough to allow the electron beam to go through. Williamson *et al.*⁶ reported that imaging of electrochemical deposition of Cu can be achieved with 5 nm resolution using an electrochemical liquid cell operated in a TEM. De Jonge *et al.*¹ was able to image biological samples through several micrometer thick water using a scanning(S) TEM. The low contrast of the biological samples was not raised as an issue since gold nanoparticles were used as markers for imaging. The thick liquid sample was not a problem either since STEM imaging mode was used and nanometer resolution was achieved. We recently developed a self-contained liquid cell, which allows real time TEM imaging of colloidal nanoparticles in liquids with subnanometer resolution^{5,7}. These newly developed liquid cells, which offer improved resolution and faster TEM imaging (30 frames per second that has not been achieved by high resolution STEM imaging), made it possible to study colloidal nanoparticle dynamics in liquids. The liquid cells fit in a standard TEM holder and can be operated as regular TEM samples. A small amount of liquid (about 30 picoliters) can be examined *in situ* under an extended chemical reaction. Various imaging and analytical (*i.e.*, energy-dispersive X-ray spectroscopy) techniques can be applied. Since the total thickness of the viewing window (including membranes and the liquid layer) can be controlled to 100 nm or below, direct imaging of biological samples (*i.e.* proteins) in liquid water without gold nanoparticle markers has also been achieved⁸.

In the past two decades, there have been significant achievements on the syntheses and applications of colloidal nanocrystals⁹⁻¹¹. However, the understanding of how nanoparticles nucleate, grow and interact with each other in liquids is largely empirical and mostly based on *ex situ* analyses¹¹⁻¹³. Our development of liquid cell TEM provides a unique platform to study the dynamic processes of nanoparticles in liquids *in situ*^{5,7,14,15}.

We fabricate a self-contained liquid cell using ultra thin silicon wafers (100 μm) by a sequential microfabrication process. It includes deposition of silicon nitride membrane, photolithographic patterning, wafer etching, spacer deposition, and cell bonding, etc. About 50 nanoliters of the reaction solution is loaded into a reservoir, which is drawn into the cell by capillary force. We fill the other reservoir with another 50 nanoliters of the liquid. Subsequently, the cell is sealed and loaded into the microscope for *in situ* imaging. Inside the microscope, the liquid sandwiched

between two silicon nitride membranes (total about 30 picoliters) can be examined. When the electron beam passes through the thin liquid layer, dynamic processes of nanoparticles in liquids can be monitored in real time. Nucleation and growth of nanoparticles can be induced by the electron beam in some cases^{5,7} or reactions can be triggered by an external heating source^{14,16}. When the electron beam damage is of a concern, low electron beam current (dose) should be used.

Since liquid cells are fabricated from silicon microfabrication processes and in large batches, variations in membrane or liquid thickness among individual liquid cells can be small⁶. Any researcher who has basic microfabrication training can successfully make liquid cells. The liquid handling technique and *in situ* TEM operation can also be mastered after practice. It is noted that besides using silicon nitride membranes as the viewing windows, other materials such as silicon dioxide, silicon or carbon (including graphene) can be used as the membrane window as well¹⁷⁻¹⁹. Since our liquid cells using small viewing windows, *i.e.*, $1 \times 50 \mu\text{m}$, no bulging of the membranes has been observed. And, the liquid cell is also robust to operate, *i.e.* below 1% of liquid cells have broken windows during the experiments. In addition, thickness of the liquid layer can also be flexibly tuned by changing the thickness of the deposited indium spacer. During sample preparation, a sealed liquid cell can maintain liquids for several days with no leakage. The small amount of liquid can be examined for several hours under the electron beam, which allows the study of an extended chemical reaction in real time.

So far, we have visualized many unique dynamic processes of nanoparticles in liquids, for example, growth and coalescence of Pt nanoparticles^{5,15}, diffusion of nanoparticles in thin liquids^{20,21}, growth fluctuation of Bi nanoparticles¹⁴, and growth of Pt₃Fe nanorods from nanoparticle building blocks⁷, etc. In addition, we have also applied this method to other areas, *e.g.*, imaging proteins in liquid water with 2.7 nm resolution⁸. In summary, our liquid cell TEM technique has been proven to be a very valuable development for the study of a wide range of fundamental issues in materials science, physics, chemistry and biology. We believe there is still large room for future technical advances and applications of the liquid TEM and it will certainly be a high impact on a broad spectrum of scientific research.

Protocol

1. Microfabrication of Liquid Cells

1. Prepare silicon wafers (p-doped, 100 μm in thickness and 4 inches in diameter) and clean the wafers using a standard wafer bath cleaning procedure.
2. Deposit low-stress silicon nitride thin films (20 nm in thickness) on both sides of the silicon wafers by low-pressure chemical vapor deposition (LPCVD) method. A custom developed recipe is used for the deposition, which allows the growth of silicon-rich nitride (SiN_x , $x < 4/3$).
3. Fabricate the bottom chip (2.6 \times 2.6 mm; 3 mm in diameter) with a viewing window (1 \times 50 μm) and the top chip (2.6 \times 2.6 mm; 3 mm in diameter) with a viewing window (1 \times 50 μm) and two reservoirs (0.6 \times 1.2 \times 0.1 mm) by following a sequence of standard fabrication processes, including photolithographic patterning, plasma etching of the SiN_x membrane (using SF_6 as the active gas), KOH wet etching of the exposed silicon wafer, etc. We use the most common photolithographic process, such as spin coating of a photoresist (positive photoresist with spin speed of 3,000 rpm for 1 min; the thickness of the photoresist is roughly 1 μm), UV exposure under the Cr mask of liquid cells, lithographic patterning using developer and fixer (deionized water), etc. There are different choices of the photoresist for spin coating and the developer for patterning. And, the corresponding parameters for the processes may also vary. Since features of the pattern are relatively large (hundreds of μm or larger), the process is easy to be accomplished. The KOH solution is prepared by dissolving potassium hydroxide power into deionized water with the potassium hydroxide:water weight ratio of 1:2. The KOH solution is maintained at 80 $^\circ\text{C}$ during etching. An etching rate of 1 μm per min can be achieved. SiN_x membrane is an ideal protective mask for KOH etching of silicon. Since etching lines are used, individual chips are connected with thin lines of etched wafer after KOH etching. Pieces of chips can be easily separated from the wafer using sharp tweezers for subsequent processes. No dicing process is needed.
4. Deposit indium spacer on the flat side of the bottom chip. First, do lithographic patterning of the chips by following the similar process in 1.3. To assist handling of the chips, stick individual chips (can be a piece of several chips) on a thin glass sheet using photoresist and let it air dry for 5 mins before spin coating, UV exposure, etc. Second, clean the patterned chips by O_2 plasma cleaning at 50 Watts for 1 min; Third, deposit indium thin film with the thickness of 100 nm on the chip by using an evaporator; Third, lift-off process is carried out to generate the indium spacer.
5. Bond the bottom and top chips together. We first align two silicon nitride viewing windows of the bottom and top chips under an optical microscope and apply a pressure of about 0.1 MPa by using a clamp. It requires practice in order to precisely align the windows on top of each other. Subsequently, liquids cells are baked in a vacuum oven at 120 $^\circ\text{C}$ for 1 hr. Lastly, we collect the cells and store the as-prepared cells in a vacuum desiccator for future usage.

The whole fabrication process is shown in **Figure 1**. We conduct all the fabrication processes at the Nanofabrication Lab of the University of California, Berkeley.

2. Preparation of Reaction Solutions

We prepare the reaction solutions for the growth Pt₃Fe nanorods as an example. Platinum (II) acetylacetonate (20 mg/ml) and Iron (II) acetylacetonate (20 mg/ml) were dissolved in a solvent mixture of pentadecane and oleylamine (7:3 vol/vol) or a mixture of pentadecane, oleylamine, and oleic acid (6:3:1 vol/vol/vol) is used for the comparison of surfactant effects.

3. Load Reaction Solutions

1. About 50 nl of reaction solution is loaded into one of the reservoirs in a liquid cell by using a syringe and Teflon nanotubes (purchased from Cole-Parmer, IL). Then, the other reservoir is filled in the same manner.

2. About 30 μl of the reaction solution is drawn into the cell by capillary force and forms a liquid layer (~ 100 nm) sandwiched between two silicon nitride membranes in the viewing window.
3. The liquid cell is subsequently sealed using a thin copper cover (~ 50 μm TEM grid with single slot 0.6 mm diameter hole, which was purchased from Tedd Pella, Inc.). Vacuum grease was applied on one-side of the cover and epoxy was used to seal the edge of the liquid cell. The total thickness of the final liquid cell is about 250-300 μm .

4. Load Liquid Cells into TEM

1. A JEOL 3010 TEM operated at 300 kV and a FEI monochromated F20 UT Tecnai operated at 200 kV are used for *in situ* imaging.
2. The liquid cell is loaded into the microscope as a standard TEM sample for imaging.

5. Real Time TEM Imaging

1. Tune the microscope to a perfect high resolution TEM imaging condition, and a beam current density of $1-8 \times 10^5$ A/m^2 is maintained during the real-time imaging.
2. For PtFe system, nucleation and growth of the nanoparticles can be initiated by casting the electron beam on the liquid layer.
3. VirtualDub software combined with Gatan DigitalMicrograph software is utilized to record the nanoparticle dynamics.

Representative Results

By using liquid cell TEM method, we have visualized the solution growth of Pt_3Fe nanorods from nanoparticle building blocks. **Figure 2** shows sequential images depicting the growth trajectory of a Pt_3Fe nanorod in different solution conditions. False coloring process using Photoshop was employed to highlight the nanoparticles.

When the solvent mixture of pentadecane and oleylamine (7:3 vol/vol) was used, three distinct stages of growth can be identified (**Figure 2A**). Firstly, many small nanoparticles are formed when the Pt and Fe precursors are reduced by electron beam irradiation. Some of them grow by monomer attachment; others undergo coalescence. Secondly, short nanoparticle chains are formed via nanoparticle interactions. Thirdly, the as-formed short nanoparticles chains act as building blocks to form relatively long winding nanoparticle chains. When a mixture of pentadecane, oleylamine, and oleic acid (6:3:1 vol/vol/vol) was used, winding nanoparticle chains are formed first, and then the nanoparticle chains straighten and form single-crystalline nanorods within a short period of time (**Figure 2B**).

In summary, we have shown the formation of single crystal nanorods via the growth of winding polycrystalline nanoparticle chains from shape-directed nanoparticle attachment followed by the straightening, orientation and shape corrections of the building blocks. Statistics and quantification of nanoparticle dynamics from the real-time imaging are of great significance to the understanding and control of hierarchical nanomaterials growth and self-assembly for functional devices⁷.

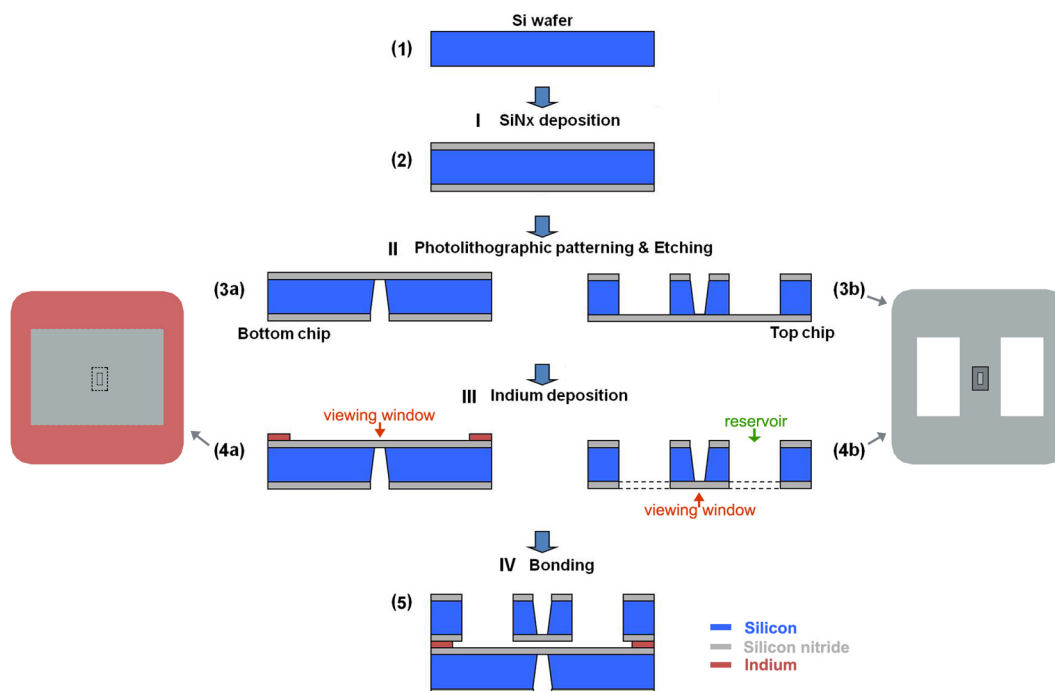


Figure 1. Overview of the microfabrication process of liquid cells. (I) Deposit silicon nitride membranes on both sides of the silicon wafer; (II) Fabricate the viewing window and reservoirs by photolithographic patterning and etching; (III) Deposit indium spacer on the flat side of the bottom chip; (IV) Bond the bottom and top chips together with a clamp.

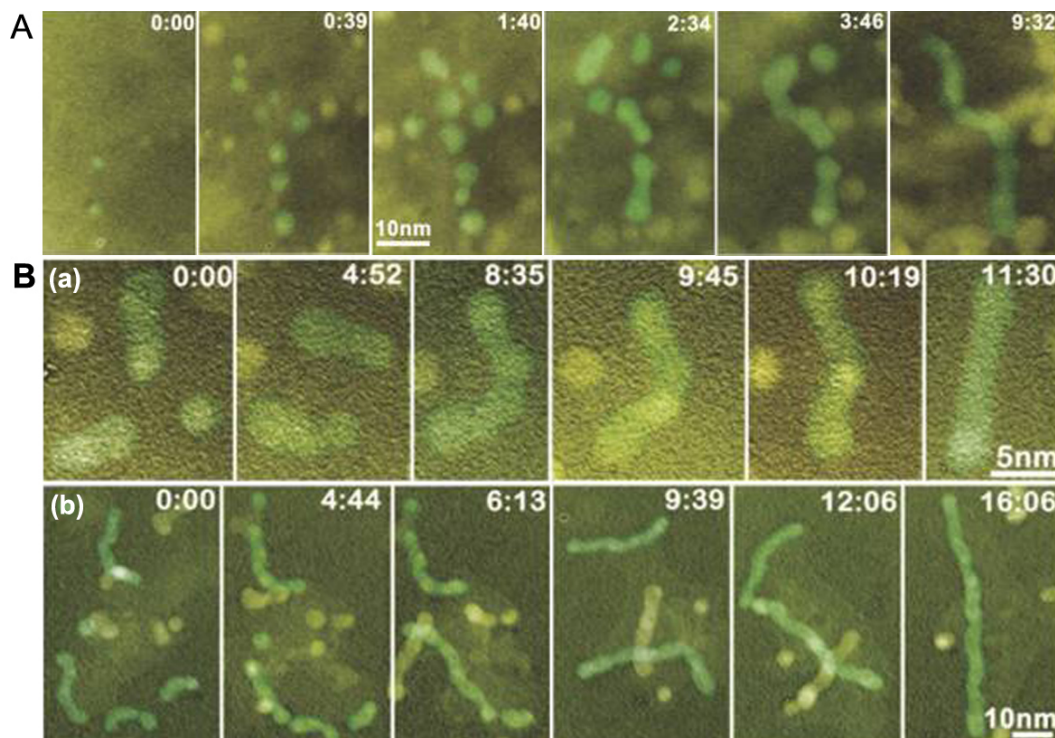


Figure 2. The growth of Pt₃Fe nanorods in a liquid cell during the exposure to electron beam. (A) Sequential TEM images showing the evolution from the initial nucleation and growth in the molecular precursor solution to a later stage of nanowire formation by shape-directed nanoparticle attachment. A solvent mixture of pentadecane and oleylamine (7:3 vol/vol) was used. (B) Formation of twisted Pt₃Fe nanorods and the subsequent straightening process. (a) Sequential TEM images of the growth of a short Pt₃Fe nanorod. (b) Sequential TEM images showing the growth of a long Pt₃Fe nanorod. A solvent mixture of pentadecane, oleylamine, and oleic acid (6:3:1 vol/vol/vol) was used. In both (A) and (B), time is displayed as min:sec, and the initial time is arbitrary⁷.

Discussion

All fabrication processes have been done in the clean room, where semiconductor devices are made.

Before the deposition of indium, O₂ plasma cleaning of the chips is necessary to eliminate the organic residue on the surface. Thus, a high quality indium spacer can be achieved, which can improve the bonding of top and bottom chips and the yield of leakage free liquid cells.

The silicon nitride viewing windows with ultrathin membrane of about 13 nm thick is a key to achieve high spatial resolution. When handling such liquid cells, special care is needed to avoid breaking the membrane during fabrication as well as experiments. For example, tweezers with a flat front are recommended. And, during the membrane cleaning process, low power and dose of O₂ plasma can be incorporated (*i.e.*, 30 W for 20-30 sec). Since growth kinetics can be highly dependent on the electron beam current density, maintaining the same electron beam current density while imaging is important. The liquid cell TEM method not only enables the study of growth dynamics of nanocrystals in solution in real time, but also allows revealing other dynamic processes (*i.e.*, diffusion of nanoparticles in liquids, liquid droplet dynamics, etc.). In addition, it provides a promising pathway to visualize biological processes in the native environment.

Disclosures

No conflicts of interest declared.

Acknowledgements

Zheng thanks Prof. A. Paul Alivisatos and Dr. Ulrich Dahmen for helpful discussions during the early development of EM liquid cells. She is grateful to the support of DOE Office of Science Early Career Research Program.

References

1. de Jonge, N. & Ross, F.M. Electron microscopy of specimens in liquid. *Nature Nanotechnology*. **6**, 695-704, doi:10.1038/nnano.2011.161 (2011).
2. Sun, Y.G. Watching nanoparticle kinetics in liquid. *Mater. Today*. **15**, 140-147 (2012).
3. Tao, F. & Salmeron, M. *In Situ* Studies of Chemistry and Structure of Materials in Reactive Environments. *Science*. **331**, 171-174, doi:10.1126/science.1197461 (2011).
4. de Jonge, N., Poirier-Demers, N., Demers, H., Peckys, D.B., & Drouin, D. Nanometer-resolution electron microscopy through micrometer-thick water layers. *Ultramicroscopy*. **110**, 1114-1119, doi:10.1016/j.ultramic.2010.04.001 (2010).
5. Zheng, H. *et al.* Observation of Single Colloidal Platinum Nanocrystal Growth Trajectories. *Science*. **324**, 1309-1312, doi:10.1126/science.1172104 (2009).
6. Williamson, M.J., Tromp, R.M., Vereecken, P.M., Hull, R., & Ross, F.M. Dynamic microscopy of nanoscale cluster growth at the solid-liquid interface. *Nature Materials*. **2**, 532-536, doi:10.1038/nmat944 (2003).
7. Liao, H.-G., Cui, L., Whitlam, S., & Zheng, H. Real-Time Imaging of Pt₃Fe Nanorod Growth in Solution. *Science*. **336**, 1011-1014, doi:10.1126/science.1219185 (2011).
8. Mirsaidov, U.M., Zheng, H., Casana, Y., & Matsudaira, P. Imaging Protein Structure in Water at 2.7 nm Resolution by Transmission Electron Microscopy. *Biophysical Journal*. **102**, L15-L17, doi:10.1016/j.bpj.2012.01.009 (2012).
9. Yin, Y.D., *et al.* Formation of hollow nanocrystals through the nanoscale Kirkendall Effect. *Science*. **304**, 711-714 (2004).
10. Kan, S., Mokari, T., Rothenberg, E., & Banin, U. Synthesis and size-dependent properties of zinc-blende semiconductor quantum rods. *Nature Materials*. **2**, 155-158, doi:10.1038/nmat830 (2003).
11. Peng, X.G., *et al.* Shape control of CdSe nanocrystals. *Nature*. **404**, 59-61 (2000).
12. Skrabalak, S.E., *et al.* Gold Nanocages: Synthesis, Properties, and Applications. *Accounts of Chemical Research*. **41**, 1587-1595, doi:10.1021/ar800018v (2008).
13. Zhang, Q.B., Xie, J.P., Yang, J.H., & Lee, J.Y. Monodisperse Icosahedral Ag, Au, and Pd Nanoparticles: Size Control Strategy and Superlattice Formation. *Acs Nano*. **3**, 139-148, doi:10.1021/nn800531q (2009).
14. Xin, H.L. & Zheng, H. *In Situ* Observation of Oscillatory Growth of Bismuth Nanoparticles. *Nano Letters*. **12**, 1470-1474, doi:10.1021/nl2041854 (2012).
15. Murray, C.B. Watching Nanocrystals Grow. *Science*. **324**, 1276-1277, doi:10.1126/science.1174666 (2009).
16. Xin, H.L., *et al.* Revealing Correlation of Valence State with Nanoporous Structure in Cobalt Catalyst Nanoparticles by *In Situ* Environmental TEM. *ACS Nano*. **6**, 4241-4247, doi:10.1021/nn3007652 (2012).
17. Daulton, T.L., Little, B.J., Lowe, K., & Jones-Meehan, J. *In situ* environmental cell transmission electron microscopy study of microbial reduction of chromium(VI) using electron energy loss spectroscopy. *Microscopy and Microanalysis*. **7**, 470-485 (2001).
18. Mohanty, N., Fahrenholtz, M., Nagaraja, A., Boyle, D., & Berry, V. Impermeable Graphenic Encasement of Bacteria. *Nano Letters*. **11**, 1270-1275, doi:10.1021/nl104292k (2011).
19. Yuk, J.M., *et al.* High-Resolution EM of Colloidal Nanocrystal Growth Using Graphene Liquid Cells. *Science*. **336**, 61-64, doi:10.1126/science.1217654 (2012).
20. Zheng, H., Claridge, S.A., Minor, A.M., Alivisatos, A.P., & Dahmen, U. Nanocrystal Diffusion in a Liquid Thin Film Observed by *In Situ* Transmission Electron Microscopy. *Nano Letters*. **9**, 2460-2465, doi:10.1021/nl9012369 (2009).
21. Park, J., *et al.* Direct Observation of Nanoparticle Superlattice Formation by Using Liquid Cell Transmission Electron Microscopy. *Acs Nano*. **6**, 2078-2085, doi:10.1021/nn203837m (2012).